

bradscholars

Equation to Line the Borders of the Folding–Unfolding Transition Diagram of Lysozyme

Item Type	Article
Authors	Mohammad, Mohammad A.;Grimsey, Ian M.;Forbes, Robert T.
Citation	Mohammad MA, Grimsey IM and Forbes RT (2016) Equation to line the borders of the folding-unfolding transition diagram of lysozyme. The Journal of Physical Chemistry B. 120(28): 6911-6916.
DOI	https://doi.org/10.1021/acs.jpccb.6b01317
Rights	This document is the Accepted Manuscript version of a Published Work that appeared in final form in The Journal of Physical Chemistry B, copyright © American Chemical Society after peer review and technical editing by the publisher. To access the final edited and published work see http://dx.doi.org/10.1021/acs.jpccb.6b01317
Download date	2026-03-09 05:53:28
Link to Item	http://hdl.handle.net/10454/8706

The University of Bradford Institutional Repository

<http://bradscholars.brad.ac.uk>

This work is made available online in accordance with publisher policies. Please refer to the repository record for this item and our Policy Document available from the repository home page for further information.

To see the final version of this work please visit the publisher's website. Access to the published online version may require a subscription.

Link to publisher's version: <http://dx.doi.org/10.1021/acs.jpcc.6b01317>

Citation: Mohammad MA, Grimsey IM and Forbes RT (2016) Equation to line the borders of the folding-unfolding transition diagram of lysozyme. *The Journal of Physical Chemistry B*. 120(28): 6911-6916.

Copyright statement: This document is the Accepted Manuscript version of a Published Work that appeared in final form in *The Journal of Physical Chemistry B*, copyright © American Chemical Society after peer review and technical editing by the publisher. To access the final edited and published work see <http://dx.doi.org/10.1021/acs.jpcc.6b01317>

1 **An Equation to Line the Borders of Folding-Unfolding Transition Diagram of Lysozyme**

2

3 Mohammad Amin Mohammad,^{*,†,‡} Ian M. Grimsey[†], and Robert T. Forbes^{†,§}

4 [†]Drug Delivery Group, School of Pharmacy, University of Bradford, Bradford BD7 1DP, UK.

5 [‡]Department of Pharmaceutics, Faculty of Pharmacy, University of Damascus, Damascus, Syria.

6 [§]School of Pharmacy and Biological Sciences, University of Central Lancashire, PR12HE, UK.

7

8 * Corresponding author

9 Dr Mohammad Amin Mohammad

10 Associate Professor in Pharmaceutical Technology

11 First name: Mohammad Amin

12 Family name: Mohammad

13 Phone: + 44 (0)1225 386797

14 Email: mam2014uk@gmail.com

15 Postal address: Dr. Mohammad Amin Mohammad, School of Pharmacy, University of Bradford,
16 Bradford, West Yorkshire, BD7 1DP, UK.

17

18 Dr Ian M. Grimsey

19 Senior Lecturer in Pharmaceutical Technology

20 Phone: +44 (0)1274 234754

21 Fax: +44 (0)1274 234769

22 i.m.grimsey@bradford.ac.uk

23 School of Pharmacy

24 University of Bradford

25 Bradford, West Yorkshire, BD7 1DP.

26

27 Prof Robert T. Forbes

28 Professor of Clinical Pharmaceutics

29 Phone: +44 (0)1772 893513

30 rtforbes@uclan.ac.uk

31 School of Pharmacy and Biomedical Sciences

32 University of Central Lancashire

33 Preston, Lancashire, PR1 2HE.

34

35

36

37

38

39

40 **ABSTRACT**

41
42 It is important for the formulators of biopharmaceuticals to predict the folding-unfolding
43 transition of proteins. This enables them to process proteins at predetermined conditions without
44 denaturation. Depending on apparent denaturation temperature (T_m) of lysozyme, we have
45 derived an equation describing its folding-unfolding transition diagram. According to water
46 content and temperature, this diagram was divided into three different areas which are the area of
47 the water-folded lysozyme phase, the area of the water-folded lysozyme phase and the bulk
48 water phase, and the area of the denatured lysozyme phase. The amount of water content
49 controlled the appearance and intensity of Raman band at $\sim 1787\text{ cm}^{-1}$ when lysozyme powders
50 were thermally denatured at temperatures higher than T_m .

51
52
53
54
55
56
57
58
59
60
61
62

63 INTRODUCTION

64

65 Protein structure and dynamics are determined by the intraprotein and protein-water non-
66 covalent interactions.^{1,2} Hydration degree of proteins, which is the weight ratio of water to
67 protein, should be ~ 0.2 to initiate protein function, moreover, full protein function requires a
68 hydration degree of ~ 1 .³ However, proteins are in their solid state during pharmaceutical
69 processes and storage. Water contents of protein powders affect their stability and performance.⁴
70 Water content alters the mechanisms of proteins' degradation reactions, and this alteration also
71 depends on other conditions such as temperature and the formulation compositions.⁵ In general,
72 increasing water content decreases the stability of protein powders. Water acts as a plasticizer
73 which enhances the molecular mobility of the proteins and so leads to an increase in their
74 degradation rates. This shortens the shelf-life of solid protein powders and formulations.

75 Many studies have used lysozyme as a model protein to understand the effect of the water
76 content on protein stability using differential scanning calorimetry (DSC). Previous works used
77 sealed DSC pans to study the effect of water content on the glass transition temperature (T_g) of
78 lysozyme, they found that T_g of lysozyme decreased by increasing the water content to approach
79 a plateau level.^{6,7} Similarly, increasing water content within lysozyme powders decreased their
80 apparent denaturation temperature (T_m) in sealed DSC pans.⁸ Therefore, both water content and
81 temperature line the borders between the native (folded) and denatured (unfolded) states of
82 lysozyme powders. These borders are important to predetermine the processing conditions (water
83 content and temperature) which preserve the native structure of proteins during manufacturing
84 processes (e.g., spray drying). Here, we derive an equation correlating water content of lysozyme
85 powders with their T_m s, and then use this equation to line the borders of the folding-unfolding

86 transition diagram of lysozyme. Also, we use Raman spectroscopy to monitor water content
87 effect on the molecular conformation of lysozyme upon the thermal unfolding transition of
88 lysozyme powders.

89

90 **EXPERIMENTAL METHODS**

91

92 **Materials.** Lyophilized hen egg-white lysozyme powder (Biozyme Laboratories, UK)
93 was purchased and considered to be unprocessed lysozyme powder.

94 **Sample Preparation.** The unprocessed lysozyme powder was used to prepare a series of
95 lysozyme powders with different water contents either by raising or reducing their water content.
96 The water residues were manipulated by exposing the powders to humidified air or to anhydrous
97 nitrogen gas for different times at 30 °C. The prepared powders were immediately sealed and left
98 to equilibrate at room temperature at least for a week after preparation. This time is enough to
99 ensure uniformity of water distribution in lysozyme particles.⁹ The prepared series of lysozyme
100 powders were tested to correlate the water content with T_m . To monitor the water content effect
101 on the molecular conformation of lysozyme upon the thermal unfolding transition, the lysozyme
102 powders with different water contents were thermally denatured inside hermetically sealed pans
103 by heating to temperatures higher than their unfolding transition peaks. These samples were
104 considered to be the thermally denatured lysozyme powders.

105 **Thermogravimetric analysis (TGA).** The water content of each powder was determined
106 using Thermo Gravimetric Analysis (TGA) (Perkin Elmer Ltd., UK). Samples (5-10 mg) were
107 heated from 30 °C to 210 °C at a scan rate of 10 °C/min in an aluminum pan under nitrogen flow
108 at 20 ml/min. Each sample was analyzed in triplicate. The decrease in the weight before

109 decomposition was considered as water content. TGA results were validated by re-analyzing the
110 water content of some samples using Karl Fischer Titration (KFT) (701 KF Titrino with 703 Ti
111 stand, Metrohm, Switzerland). Using TGA instead of KFT as only a few mg is enough for TGA.

112 **Differential scanning calorimetry (DSC).** T_m of each sample was measured using
113 Differential Scanning Calorimetry (DSC) (Perkin-Elmer Ltd., UK). To study the effect of water
114 residue on the thermal stability of lysozyme (the value of T_m), the evaporation of water during
115 heating was suppressed by using Large Volume Capsules, which are stainless steel sample
116 containers equipped with an O-ring seal to provide a hermetic seal. Lysozyme powders (5-10mg)
117 and solutions in water (20 μ l) were encapsulated in the hermetically sealed pans and scanned
118 between 40 °C to 200 °C at 5 °C/min in triplicate. DSC was also used to prepare the thermally
119 denatured lysozyme powders by heating them inside the hermetically sealed pans to temperatures
120 higher than their unfolding transitions.

121 **FT-Raman spectroscopy.** FT-Raman spectra of the lysozyme powders at different water
122 content and their thermally denatured lysozyme counterpart powders were recorded with a
123 Bruker IFS66 optics system using a Bruker FRA 106 Raman module. The excitation source was
124 an Nd: YAG laser operating at 1064 nm and a laser power of 50 mW was used. The FT-Raman
125 module is equipped with a liquid nitrogen cooled germanium diode detector with an extended
126 spectrum band width covering the wave number range 1850-1100 cm^{-1} . Samples were placed in
127 stainless steel sample cups and scanned 200 times with the resolution set at 8 cm^{-1} . The observed
128 band wave numbers were calibrated against the internal laser frequency and are correct to better
129 than $\pm 1 \text{ cm}^{-1}$. The spectra were corrected for instrument response. The experiments were run at a
130 controlled room temperature of $20 \pm 1^\circ\text{C}$.

131

132 **Results and discussion**

133

134 We employed this protein because it folds in a highly cooperative manner and so exhibits
135 an all-or-none thermal unfolding transition, and so it displayed one denaturation peak, in solid
136 and solution states,^{10,11} which makes the study easier. The driest prepared lysozyme powder
137 contained 2.6 ± 0.1 %w/w water and its T_m was 436.9 ± 0.6 K, while the wettest powder contained
138 20.3 ± 2.3 %w/w water and its T_m was 355.5 ± 3.1 K. In Figure 1 is a DSC thermogram of each
139 sample, showing an inverse correlation between water content and T_m s.

140

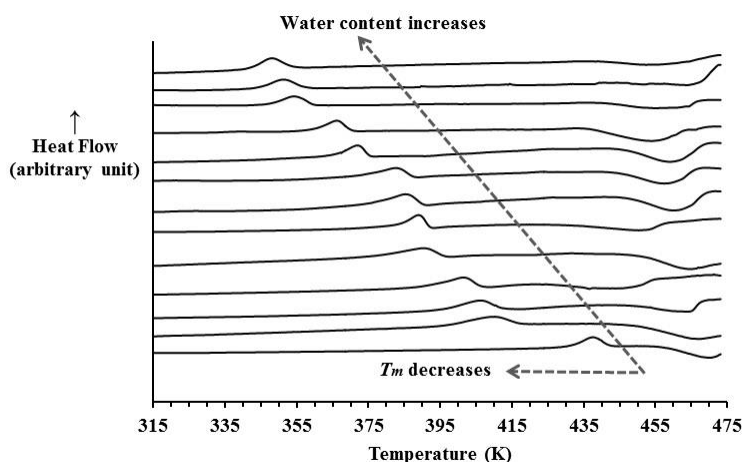


Figure 1. Differential scanning calorimetry thermograms of lysozyme powders (in sealed pans) at different water content.

141

142 Previous study demonstrated that DSC thermograms of lysozyme powders with different
143 water content performed in pierced pans showed two endothermic peaks, the first broad peak,
144 which extends from ~ 298 to 433 K, indicates water evaporation and its area directly correlates to
145 the water content, the second peak at ~ 473 K refers to the protein denaturation (T_m) and its

146 position is independent of water content because water evaporates through the pierced pans
147 before the unfolding transition (denaturation) of lysozyme.¹⁰

148 However, unlike the experiments performed in the pierced pan, Figure 1 shows that the
149 position of the endothermic unfolding peak (T_m) varied for different water contents when DSC
150 experiments were performed under sealed conditions. The DSC thermograms (Figure 1) did not
151 show the water evaporation peak because the evaporation of water during heating was
152 suppressed by the hermetical seal, i.e., the pressure generated from increasing the temperature of
153 the air, which had been trapped during the capsulation of the hermetically sealed pans, prevented
154 water loss. Figure 1 also show an exothermic peak after lysozyme unfolding in all samples
155 analysed with the sealed pans. This peak was reproducible and showed little variation between
156 samples, with a peak position ranging from 453 to 468 K. It was believed that this exothermic
157 peak could be due to the aggregation of lysozyme molecules after unfolding, however re-
158 scanning the sealed pans containing previously aggregated lysozyme powders also gave an
159 exothermic peak at the same position but without the endothermic unfolding peak.

160 We hypothesized that water molecules associate with lysozyme powders to form a
161 homogenous water-folded lysozyme phase. This phase unfolds at a kinetic thermal energy
162 depending on water mole fraction (X_w) and lysozyme mole fraction (X_p) within the powders.
163 When X_w increases, T_m of the unfolding kinetic energy is reduced, and its reduction stops when
164 the water molecules reach their saturation limit within the water-folded lysozyme phase. Above
165 this limit, water molecules segregate from the water-folded lysozyme phase to form another
166 phase of bulk water, and so they cannot reduce T_m further.

167 X_w / X_p equals N, the ratio of water molecules to lysozyme molecules, and it is calculated
168 according to Eq. (1):

169
$$N = 14296 \times W\%/18 \times P\% \quad (1)$$

170 18 and 14296 are the molecular weights of water and lysozyme, respectively, and W% and P%
 171 are the percentage of water weight and protein weight in the powders, respectively. The results
 172 were tabulated in Table 1.

173

Table 1. The apparent denaturation temperature (T_m), number of water molecules associating with one lysozyme molecule (N), water mole fraction (X_w) and lysozyme mole fraction (X_p) of lysozyme powders at different water content.

Water content % w/w	T_m (K)	N	X_w	X_p
2.5 (0.1)	436.9 (0.6)	20.4	0.9532	0.0468
4.6 (0.3)	412.0 (1.6)	38.1	0.9744	0.0256
5.2 (0.1)	406.2 (2.1)	43.4	0.9775	0.0225
6.4 (0.2)	401.9 (1.4)	54.3	0.9819	0.0181
7.7 (0.1)	390.3 (0.2)	66.6	0.9852	0.0148
8.5 (0.1)	388.8 (2.6)	73.8	0.9866	0.0134
9.2 (0.5)	385.5 (0.3)	80.5	0.9877	0.0123
9.9 (0.1)	383.5 (0.6)	87.7	0.9887	0.0113
12.0 (0.1)	371.8 (0.4)	108.7	0.9909	0.0091
14.4 (0.1)	365.7 (0.4)	133.1	0.9925	0.0075
15.6 (0.6)	364.0 (1.6)	146.6	0.9932	0.0068
20.3 (2.3)	355.5 (3.1)	201.8	0.9951	0.0049

Values within parenthesis are standard deviation, n = 3.

174

175 T_m reflects the value of thermal kinetic energy needed to overcome the cohesion energy
 176 stabilizing the folded state of proteins. This cohesion energy results from Van der Waals
 177 attraction, electrostatic interaction, hydrogen bonding, and conformational entropy (hydrophobic
 178 effect).¹² Electrostatic and hydrophobic interactions play the main roles in protein folding.^{1,13}
 179 Water affects these interactions and hence the magnitude of T_m needed to unfold proteins. Water
 180 molecules surround the surface of protein molecules and penetrate into their cavities.¹⁴
 181 Surrounding water molecules strengthen the hydrophobic effect by an increase in the entropy of
 182 water due to association between hydrophobic residues.¹³ However, according to Coulomb's law,

183 the interior waters weaken the electrostatic forces because they increase the dielectric constant in
 184 the interior of protein molecules and also increase the distances between polarized and ionized
 185 groups of proteins.^{15,16} Our results demonstrated that the net effect of water weakens the forces
 186 responsible for the folded state, and so the increased water content facilitates the protein
 187 unfolding at lower T_m . Dehydration of lysozyme powders stabilizes its native form because the
 188 free energy change of the lysozyme denaturation increases by dehydration.¹⁷

189 Multiplying the gas constant (R) by T_m gives the kinetic thermal energy needed to unfold
 190 lysozyme. Interestingly, our data (Table 1) prove that RT_m and $\ln N$ correlate linearly with a
 191 correlation coefficient close to one ($r = -0.997$), and their linear equation is:

$$192 \quad \ln N = \text{Slope } RT_m + \text{Intercept} \quad (2)$$

193 Figure 2 shows the straight line of Eq. (2) which was regressed in Eq. (3).

$$194 \quad \ln N = -\frac{RT_m}{72.3} + 15.0 \quad (3)$$

195 where 72.3 has units of Cal.mole^{-1} and 15.0 has units of mole.mole^{-1} (i.e., unitless). $R =$
 196 $1.9872041 \text{ Cal.mole}^{-1}.\text{K}^{-1}$, therefore Eq. (3) can be reduced to Eq. (4):

$$197 \quad T_m = -36.4 \ln N + 545.7 \quad (4)$$

198

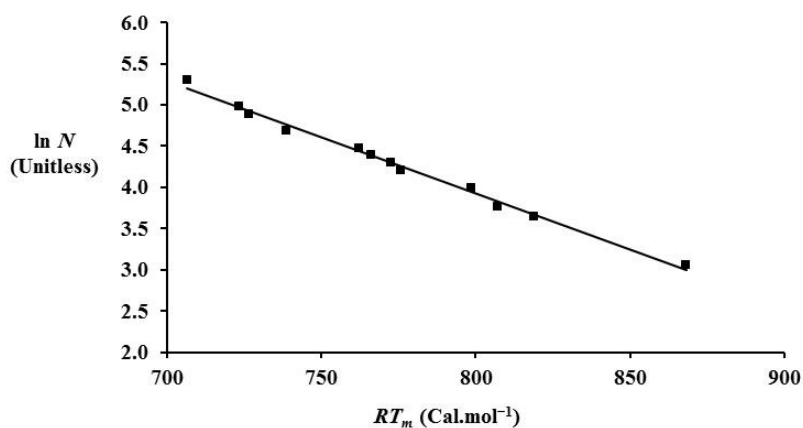


Figure 2. The linear correlation between the denaturation thermal kinetic energy and logarithm of water molecules associating with one lysozyme molecule.

199 We measured T_m s of lysozyme solutions containing 80 %w/w and 70 %w/w of water.
200 T_m s of the solutions were 348.2 ± 0.7 and 348.0 ± 1.0 K, respectively, and they were similar (T-
201 test: $P < 0.05$). According to our hypothesis, T_m of the lysozyme solutions equals the apparent
202 denaturation temperature of the saturated water-lysozyme phase (T_m^S). Therefore, we extrapolated
203 Eq. (4) to T_m^S (348K), which is the same as that of the solutions, to calculate the number of water
204 molecules which saturate one molecule of lysozyme (N^S) as follows:

$$205 \quad T_m^S = -36.4 \ln N^S + 545.7 \quad (5)$$

206 The calculated N^S was 228 water molecules according to Eq. (5). This water amount is
207 equivalent to 22.3 %w/w and 0.3 g/g protein. We then prepared another lysozyme powder with a
208 water content of 23.2 ± 1.1 %w/w, which is similar to the calculated N^S . T_m of the prepared water
209 saturated powder was 347.8 ± 1.4 K, which is similar to T_m^S (T-test: $P < 0.05$). Therefore, we used
210 temperature and N to draw the folding-unfolding transition diagram of lysozyme. Figure 3 shows
211 this diagram in which the denaturation line obeys Eq. (3) until reaching the water saturated solid
212 state at N^S . After this value of water molecules, T_m did not significantly change. Our calculated
213 value of N^S , i.e. 228 water molecules, is similar to previously reported values of the hydration
214 shell of lysozyme. Previous researchers used gigahertz to terahertz spectroscopy^{18,19} Raman
215 spectroscopy²⁰ neutron and X-ray scattering²¹ NMR²² to quantitate the hydration shell of
216 lysozyme, and these methods estimated similar values of the hydration shell of lysozyme, and the
217 values ranged between 170-270 water molecules. Hydration shell molecules have different
218 properties from bulk water.²³ Our results demonstrate that the effect of water molecules on T_m
219 changed at $N > N^S$. Therefore, we speculate that water molecules begin to form the bulk water at
220 $N > N^S$. Therefore, the folding-unfolding transition diagram of lysozyme (As shown in Figure 3)
221 was divided to three areas; (A) represents the area of the water-folded lysozyme phase, (B)

222 represents the area of the water-folded lysozyme phase and the bulk water phase, and (C)
223 represents the area of the denatured lysozyme phase, and the line separating (C) from (A) and
224 (B) is the denaturation line.
225

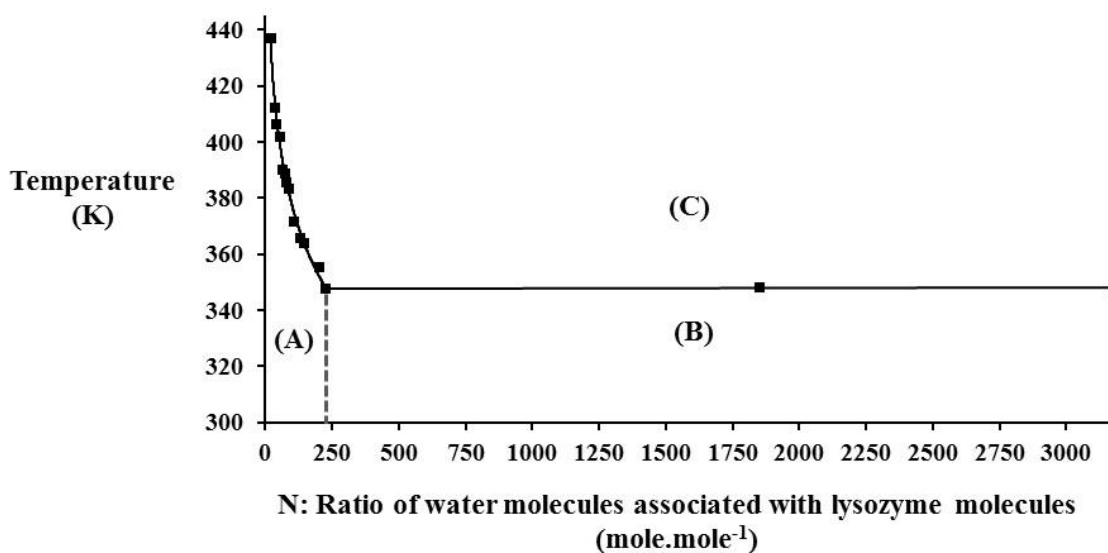


Figure 3. The folding-unfolding transition diagram of lysozyme. (A) represents the area of the water-folded lysozyme phase, (B) represents the area of the water-folded lysozyme phase and the bulk water phase, and (C) represents the area of the denatured lysozyme phase; the line separating (C) from (A) and (B) is the denaturation line.

226
227 Although T_m of lysozyme solutions is usually ~ 348 K, it changes due to additives (e.g.,
228 co-solvents, pH, ionic strength).^{10,24,25} Also, additives changed T_m of lysozyme powders.⁸ We
229 could conclude that if the additives are miscible with water, they will participate in forming
230 water-protein phases (in both solid and solution states). Therefore, they would change the
231 constants of Eqs. (3) and (5). Whilst other proteins may have different constants.

232 Previous Raman study clarified the significant effects of hydration degree of native
233 lysozyme powders on the back bone and the side chain conformations of lysozyme.⁹ In other
234 words, this previous study covered the molecular conformation of lysozyme under the

235 denaturation line of the folding-unfolding transition diagram of lysozyme. Here, the molecular
236 conformation of lysozyme above the denaturation line were investigated. Raman spectra of the
237 thermally denatured powders at different hydration degree and their original powders were
238 collected at room temperature and presented in Figure 4. The peak intensities of the spectra were
239 normalized using the band at 1447 cm^{-1} (CH bending) as internal intensity standard. This is
240 because its intensity and position are unaffected by changes induced in protein structure after
241 applying different stresses.²⁶

242

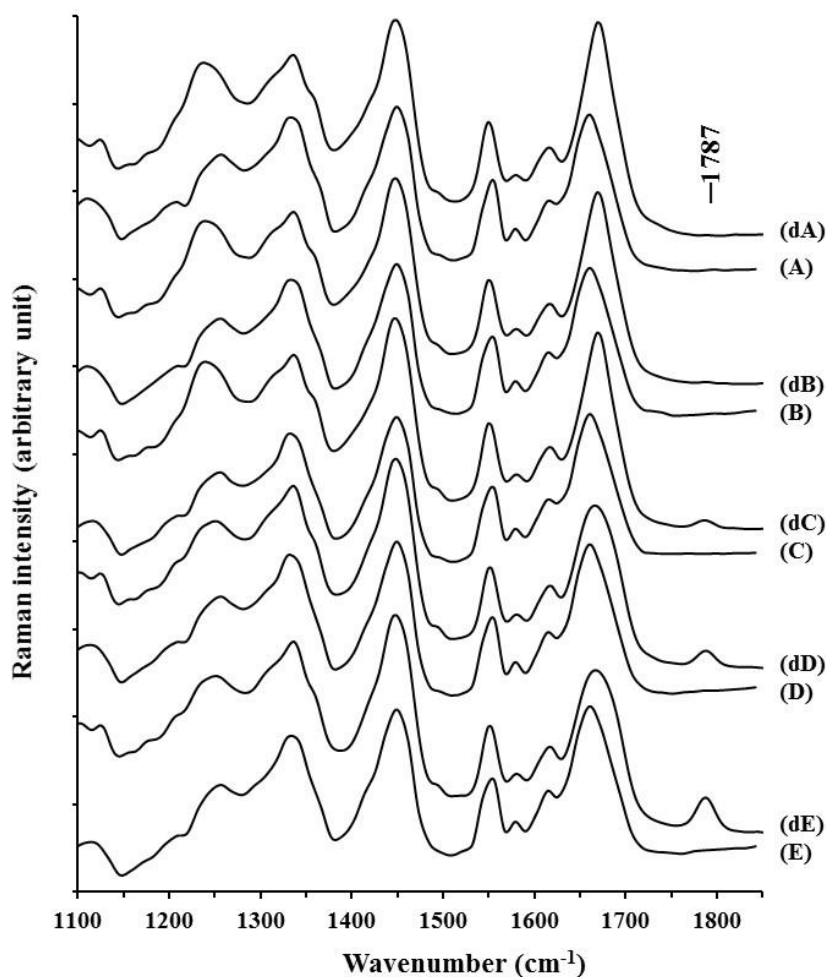


Figure 4. Representative Raman spectra of lysozyme powders in the $1100\text{--}1850\text{ cm}^{-1}$ wavenumber region, (A), (B), (C), (D) and (E) represent lysozyme powders at different water content of 20.3, 12.0, 8.2, 5.2 and 2.5 %w/w, respectively, and (dA), (dB), (dC), (dD) and (dE)

represent their thermally denatured counterpart powders (in sealed pans), respectively.

243 Within the investigated wavenumber region (1100–1850 cm^{-1}), we did not notice
244 significant differences between the studied original lysozyme samples (Figure 4, spectra A, B, C,
245 D and E). However, compared to the original lysozyme powders, the Raman spectra of the
246 counterpart thermally denatured powders showed changes in the the peak positions of amide I
247 and amide III bands. The peak of amide I was upshifted from ~ 1660 to ~ 1671 cm^{-1} after thermal
248 denaturation (Figure 4, spectra dA, dB, dC, dD and dE), and also spectra dD and dE show
249 broadening in the amide I band in the case of the thermally denatured samples at low hydration
250 degree (5.2 and 2.5 % w/w). The peak of amide III was downshifted from ~ 1256 to ~ 1249 cm^{-1} at
251 low hydration degree (spectra dD and dE), and it was further downshift to ~ 1240 cm^{-1} with an
252 increase in the intensity at higher hydration degree (spectra dA, dB and dC). The Raman Bands
253 of the amide I (C=O stretch) and amide III (N-H in-plane bend + C-N stretch) are indicators of
254 the protein's secondary structures.⁹ The mid-point of amide I is expected to be at 1665 ± 5 cm^{-1}
255 for α -helix and 1670 ± 3 cm^{-1} for β -sheet and disordered secondary structure, and the mid-point of
256 amide III is expected to be at 1267 ± 8 cm^{-1} for α -helix, 1235 ± 5 cm^{-1} for β -sheet and 1245 ± 4 cm^{-1}
257 for disordered structure.^{27,28} Therefore, the changes in Raman bands (presented in Figure 4)
258 indicate that the content of the β -sheet and disordered secondary structure were increased and at
259 the same time the α -helix content was decreased after the thermal denaturation. Similar changes
260 in the positions of amide I and amide III Raman bands of lysozyme powders were reported when
261 lysozyme powders were denatured using mechanical stress¹⁰ and γ -radiation²⁹, and the
262 researchers attributed these changes to a decrease in the α -helix with an increase in the β -sheet
263 and disordered structures. However, in the case of the thermally denatured powders, a new
264 Raman band at ~ 1787 cm^{-1} appeared, and its intensity decreased by raising the water content

265 (Figure 4, spectra dC, dD and dE), and the peak disappeared at water content ≥ 12 %w/w (Figure
266 4, spectra dA and dB). Therefore, the appearance of this peak at 1787 cm^{-1} relates to the nature
267 of lysozyme molecules' movement during the thermal unfolding transition and this movement
268 depends heavily on the amount of hydration degree of the powders. The new band at 1787 cm^{-1}
269 could be assigned to the stretching of free hydrogen bonding carbonyl group. As the line of
270 amide I at wavenumbers $\geq 1685\text{ cm}^{-1}$ is expected to be assigned to the disordered secondary
271 structure without hydrogen bonding.²⁷ It can be concluded that the higher the water content in
272 lysozyme powders during unfolding transition, the higher the freedom for lysozyme molecules to
273 move and saturate the free carbonyl groups of the peptide bonds resulted from the unfolding
274 transition. At water content ≥ 12 %w/w, the lysozyme molecules have enough freedom to move
275 and saturated all the free carbonyl groups, and this explains the disappearance of the Raman band
276 at 1787 cm^{-1} . This finding agrees with previous results stating that at water content between 11
277 and 21 %w/w, lysozyme possess a glasslike dynamic transition from rigid to flexible state due to
278 the mobility increase of the structural units.³⁰

279 Therefore, the shape of amide I Raman band, the position and intensity of amide III
280 Raman band, and the intensity of the Raman band at $\sim 1787\text{ cm}^{-1}$ of the thermally denatured
281 powders depend on the water content of their original native powders. This indicates that the
282 molecular structure of the thermally denature lysozyme depends on its hydration degree.

283 This folding-unfolding transition diagram of lysozyme was obtained using sealed pans in
284 order to ensure mass conservation of the water-lysozyme system. Therefore, it was determined at
285 constant volume but variable pressure. Fortunately, in our case, we capsulated the sealed pans at
286 atmospheric pressure ($\sim 0.1\text{MPa}$), and according to the general gas law, the increase in the
287 pressure due to the temperature increase from 298 to 473 K inside the hermetically sealed pans

288 would reach ~0.2 MPa. This pressure values have a negligible role in the lysozyme denaturation.
289 It was confirmed that lysozyme is denatured when pressure is at much higher values >500
290 MPa.³¹

291

292 **CONCLUSIONS**

293

294 These results allowed us to derive an equation correlating T_m of lysozyme with its
295 hydration degree. T_m exponentially decreased when the hydration degree increased, and it did
296 not significantly decrease further after hydration degree reaching a value similar to hydration
297 shell of the lysozyme. We used the derived equation to draw the folding-unfolding transition
298 diagram of lysozyme. This diagram will be useful to process lysozyme at predetermined
299 conditions of temperature and water content without denaturation. The molecular conformation
300 of the thermally denatured lysozyme was found to be dependent on the hydration degree of the
301 original native powders. A new Raman band at 1787 cm^{-1} appeared in the spectra of the
302 thermally denatured lysozyme, and its intensity reversibly correlated with the water content and
303 it disappeared at the water content $\geq 12\text{ %w/w}$.

304

305 **AUTHOR INFORMATION**

306 Corresponding Author

307 *E-mail: mam2014uk@gmail.com

308 Notes

309 The authors declare no competing financial interest.

310

311

312 **ACKNOWLEDGEMENTS**

313

314 The authors thank Dr Ian S. Blagbrough (University of Bath) for helpful discussions.
315 MAM gratefully acknowledges CARA (Stephen Wordsworth and Ryan Mundy) and University
316 of Bradford for providing an academic fellowship.

317

318 **REFERENCES**

- 319 (1) Ji, C.; Mei, Y. Some practical approaches to treating electrostatic polarization of proteins.
320 *Acc. Chem. Res.* 2014, *47*, 2795–2803.
- 321 (2) Dhindsa, G. K.; Tyagi, M.; Chu, X. Q. Temperature-dependent dynamics of dry and hydrated
322 beta-casein studied by quasielastic neutron scattering. *J. Phys. Chem. B* 2014, *118*, 10821–
323 10829.
- 324 (3) Frauenfelder, H.; Chen, G.; Berendzen, J.; Fenimore, P. W.; Jansson, H.; McMahon, B. H.;
325 Stroe, I. R.; Swenson, J.; Young, R. D. A unified model of protein dynamics. *Proc. Natl. Acad.*
326 *Sci. U.S.A.* 2009, *106*, 5129–5134.
- 327 (4) Broadhead, J.; Rouan, S. K.; Hau, I.; Rhodes, C. T. The effect of process and formulation
328 variables on the properties of spray-dried beta-galactosidase. *J. Pharmacol. Pharmacother.* 1994,
329 *46*, 458–467.
- 330 (5) Wang, W. Lyophilization and development of solid protein pharmaceuticals. *Int. J. Pharm.*
331 2000, *203*, 1–60.
- 332 (6) Miyazaki, Y.; Matsuo, T.; Suga, H. Low-temperature heat capacity and glassy behavior of
333 lysozyme crystal. *J. Phys. Chem. B* 2000, *104*, 8044–8052.
- 334 (7) Panagopoulou, A.; Kyritsis, A.; Aravantinou, A. M.; Nanopoulos, D.; Serra, R. S. I.; Ribelles,
335 J. L. G.; Shinyashiki, N.; Pissis, P. Glass transition and dynamics in lysozyme-water mixtures
336 over wide ranges of composition. *Food Biophys.* 2011, *6*, 199–209.
- 337 (8) Bell, L. N.; Hageman, M. J.; Muraoka, L. M. Thermally induced denaturation of lyophilized
338 bovine somatotropin and lysozyme as impacted by moisture and excipients. *J. Pharm. Sci.* 1995,
339 *84*, 707–712.
- 340 (9) Kocherbitov, V.; Latynis, J.; Misiunas, A.; Barauskas, J.; Niaura, G. Hydration of lysozyme
341 studied by Raman spectroscopy. *J. Phys. Chem. B* 2013, *117*, 4981–4992.
- 342 (10) Mohammad, M. A.; Grimsey, I. M.; Forbes, R. T. Mapping the solid-state properties of
343 crystalline lysozyme during pharmaceutical unit-operations. *J. Pharm. Biomed. Anal.* 2015, *114*,
344 176–183.
- 345 (11) Maroufi, B.; Ranjbar, B.; Khajeh, K.; Naderi-Manesh, H.; Yaghoobi, H. Structural studies
346 of hen egg-white lysozyme dimer: comparison with monomer. *Biochim. Biophys. Acta* 2008,
347 *1784*, 1043–1049.
- 348 (12) Yano, Y. F. Kinetics of protein unfolding at interfaces. *J. Phys. Condens. Matter* 2012, *24*,
349 503101–503117.

- 350 (13) Wu, Z.; Cui, Q.; Yethiraj, A. Driving force for the association of hydrophobic peptides: the
351 importance of electrostatic interactions in coarse-grained water models. *J. Phys. Chem. Lett.*
352 2011, 2, 1794–1798.
- 353 (14) Tilton, R. F. Jr.; Kuntz, I. D. Jr.; Petsko, G. A. Cavities in proteins: Structure of a
354 metmyoglobin xenon complex solved to 1.9 Å. *Biochemistry* 1984, 23, 2849–2857.
- 355 (15) Dwyer, J. J.; Gittis, A. G.; Karp, D. A.; Lattman, E. E.; Spencer, D. S.; Stites, W. E.;
356 García-Moreno E, B. High apparent dielectric constants in the interior of a protein reflect water
357 penetration. *Biophys. J.* 2000, 79, 1610–1620.
- 358 (16) Pitera, J. W.; Falta, M.; Van Gunsteren, W. F. Dielectric properties of proteins from
359 simulation: the effects of solvent, ligands, pH, and temperature. *Biophys. J.* 2001, 80, 2546–2555.
- 360 (17) Kocherbitov, V.; Arnebrant, T. Hydration of thermally denatured lysozyme studied by
361 sorption calorimetry and differential scanning calorimetry. *J. Phys. Chem. B* 2006, 110, 10144–
362 10150.
- 363 (18) Vinh, N. Q.; Allen, S. J.; Plaxco, K. W. Dielectric spectroscopy of proteins as a quantitative
364 experimental test of computational models of their low-frequency harmonic motions. *J. Am.*
365 *Chem. Soc.* 2011, 133, 8942–8947.
- 366 (19) Knab, J.; Chen, J. Y.; Markelz, A. Hydration dependence of conformational dielectric
367 relaxation of lysozyme. *Biophys. J.* 2006, 90, 2576–2581.
- 368 (20) Bellavia, G.; Paccou, L.; Achir, S.; Guinet, Y.; Siepmann, J.; Hédoux, A. Analysis of Bulk
369 and Hydration Water During Thermal Lysozyme Denaturation Using Raman Scattering. *Food*
370 *Biophys.* 2013, 8, 170–176.
- 371 (21) Svergun, D. I.; Richard, S.; Koch, M. H. J.; Sayers, Z.; Kuprin, S.; Zaccai, G. Protein
372 hydration in solution: experimental observation by x-ray and neutron scattering. *Proc. Natl.*
373 *Acad. Sci. U.S.A.* 1998, 95, 2267–2272.
- 374 (22) Kuntz, I. D. Hydration of macromolecules. III. Hydration of polypeptides. *J. Am. Chem.*
375 *Soc.* 1971, 93, 514–516.
- 376 (23) Choudhuri, J. R.; Chandra, A. An ab initio molecular dynamics study of the hydrogen
377 bonded structure, dynamics and vibrational spectral diffusion of water in the ion hydration shell
378 of a superoxide ion. *Chem. Phys.* 2014, 445, 105–112.
- 379 (24) Blumlein, A.; McManus, J. J. Reversible and non-reversible thermal denaturation of
380 lysozyme with varying pH at low ionic strength. *Biochim. Biophys. Acta. Proteins and*
381 *Proteomics* 2013, 1834, 2064–2070.
- 382 (25) Chen, P.; Seabrook, S. A.; Epa, V. C.; Kurabayashi, K.; Barnard, A.S.; Winkler, D. A.;
383 Kirby, J. K.; Ke, P. C. Contrasting effects of nanoparticle binding on protein denaturation. *J.*
384 *Phys. Chem. C* 2014, 118, 22069–22078.
- 385 (26) Yu, T. J.; Lippert, J. L.; Peticolas, W. L. Laser Raman studies of conformational variations
386 of poly-L-lysine. *Biopolymers* 1973, 12, 2161–2176.
- 387 (27) Li-Chan, E. C. Y. The applications of Raman spectroscopy in food science.
388 *Trends. Food. Sci. Tech.* 1996, 7, 361–370.
- 389 (28) Yu, N. T.; Liu, C. S. Laser Raman Spectra of Crystalline and Aqueous Glucagon. *J. AM.*
390 *Chem. Soc.* 1972, 94, 5127–5135.
- 391 (29) Torreggiani, A.; Tamba, M.; Manco, I.; Faraone-Mennella, M. R.; Ferreri, C.;
392 Chatgililoglu, C. Radiation damage of lysozyme in a biomimetic model: some insights by
393 Raman spectroscopy. *J. Mol. Struct.* 2005, 744, 767–773.
- 394 (30) Kocherbitov, V.; Arnebrant, T.; Söderman, O. Lysozyme–water interactions studied by
395 sorption calorimetry. *J. Phys. Chem. B* 2004, 108, 19036–19042.

396 (31) Hédoux, A.; Guinet, Y.; Paccou, L. Analysis of the mechanism of lysozyme pressure
397 denaturation from Raman spectroscopy investigations, and comparison with thermal
398 denaturation. *J. Phys. Chem. B* 2011, *115*, 6740–6748.

399 **TOC GRAPHICS**

$$T_m = -36.4 \ln N + 545.7 \text{ when } N \leq N^S$$

$$T_m \cong T_m^S \text{ when } N \geq N^S$$

T_m : Apparent denaturation temperature
of lysozyme.

N: Ratio of water molecules to lysozyme
molecules.

S: Superscript refers to saturated
water-lysozyme state.

400